Hardening and softening mechanisms at decreasing microstructural length scales

Carl Fredrik Oscar Dahlberg, Peter Gudmundson

Hardening and softening mechanisms at decreasing microstructural length scales

Journal:	*Philosophical Magazine & Philosophical Magazine Letters*
Manuscript ID:	TPHM-07-Nov-0323.R2
Journal Selection:	Philosophical Magazine
Date Submitted by the Author:	24-Feb-2008
Complete List of Authors:	Dahlberg, Carl; Royal Institue of Technology (KTH), Solid Mechanics Gudmundson, Peter; Royal Institute of Thechnology (KTH), Solid Mechanics
Keywords:	constitutive equations, grain boundary interfaces, interfaces, mechanical properties, nanograined structures, plasticity, strengthening mechanisms
Keywords (user supplied):	Inverse Hall-Petch effect
Note: The following files were submitted by the author for peer review, but cannot be converted to PDF. You must view these files (e.g. movies) online.	
DahlbergGudmundsonIUTAM07.tex	

Philosophical Magazine,
Vol. 00, No. 00, DD Month 2008, 1–11

Hardening and softening mechanisms at decreasing microstructural length scales

CARL F. O. DAHLBERG* and PETER GUDMUNDSON

Department of Solid Mechanics, Royal Institute of Technology, KTH, SE-100 44 Stockholm, Sweden

(February 2008)

A laminate structure with varying laminae thicknesses is used as a qualitative model of grain size dependence on yield behaviour in metallic materials. Both strain gradient plasticity and slip between layers are considered. It is shown that an inverse Hall–Petch effect can be generated in this way. For very small thicknesses, corresponding to very small grain sizes, sliding is the dominating mechanism and the strength then decreases with decreasing thickness. For larger thicknesses, strain gradient plasticity is controlling the deformation and the strength is instead increasing with decreasing thickness. Numerical examples are presented that demonstrate these mechanisms.

Keywords: Strain gradient plasticity; Inverse Hall–Petch effect; Bulk/Interface competition; Intergrain boundary sliding

1 Introduction

There is today substantial evidence that the mechanisms of plastic deformation changes with the length scale of the problem at hand. When decreasing the length scale several investigations have shown that the strength generally increases. The increase in strength with decreasing grain sizes is denoted as the Hall–Petch effect. There are however many other experiments that have shown an increase in strength with decreasing structural length scales. A few examples are results from torsion of thin wires [1], bending of thin beams [2] and experiments on thin films [3–5].

When the length scale of the problem drops even further, other mechanisms need to be involved to account for the experimental evidence that shows less and less hardening and even softening at really small length scales. This is typically referred to as the inverse Hall–Petch effect in nanocrystalline solids and has been reported in [6–8], amongst others. These results have lately been confirmed by molecular dynamics simulations [9–12]. Thus adding to the indication that a reversal of the slope in the Hall–Petch relationship is possible at diminished length scales. This in turn means that there exists a maximum yield strength at some intermediate length scale.

Material scientists have since long been able to view many of the finer intricacies in the process of plastic deformation as it takes place. Thereby they have contributed with a lot of necessary knowledge on the physical processes that lie behind the phenomenon of plastic deformation. This knowledge is based on the understanding of crystalline solids and the theory of dislocations. Albeit there is still much left to understand and conclude within this field, one of the real challenges that remains are in the hands of the continuum mechanical community. There is a strong need to formulate a consistent, and preferably simple, theory that enable accurate predictions on the micro- and nano-level.

Several theories have been suggested in the literature. The theory adopted in this paper is the higher-order strain gradient theory by Gudmundson, first reported in [13], and further investigated in articles by Fredriksson and Gudmundson [14–16]. This theory shares many common features with several other theories presented in the literature [17–20]. There are also a family of so called lower-order theories of strain gradient plasticity, for example [21], which predict the same kind of behaviour as higher-order theories in the presence of an inhomogeneous strain field. In the case of simple shear loading the strain field would be homogeneous and there would be no way to model the development of a gradient in relation to a

*Corresponding author. Email: carl@hallf.kth.se

Philosophical Magazine
ISSN 0950-0839 print/ISSN 1362-3036 online
http://www.tandf.co.uk/journals
DOI: 10.1080/0950083YYxxxxxxxx

boundary layer in the strained material since these lower-order theories do not allow for the formulation of higher-order boundary conditions.

Most of these strain gradient theories introduce one or several length scales by considering the contributions of the strain gradients in the formulation of the principle of internal virtual work. Some of these models are mainly phenomenological in spirit, while others connect the gradient of plastic strain to the density of geometrically necessary dislocations. They can account for the increase in yield strength due to the increased density of geometrically necessary dislocations in micro grain size materials by taking into account the non-local effects of an inhomogeneous plastic strain field. On the other hand, they lack the ability to describe the aforementioned decrease in yield strength in materials with nano-sized grains. This is thought to be due to a change in plastic deformation mechanism occurring at really small length scales, which will fall outside of the predictive abilities of these theories unless another mechanism altogether is considered and introduced.

In the present paper, grain boundary sliding is introduced as a competing mechanism. It is shown that this mechanism is dominant at the smallest length scales and that it causes a softening behaviour. Numerical simulations of a laminated structure are used to demonstrate the competition between hardening and softening due to strain gradient plasticity and sliding respectively.

2 Theory

The gradient plasticity theory used in this article is the theory presented in [13], and it will here only be given as a brief introduction. It is a so called higher-order theory, which means that the gradients of plastic strain are assumed to contribute to the work per unit volume. This will have the effect of contributions from the plastic strains and the gradients thereof when formulating the principle of virtual work.

2.1 *Governing equations*

The internal virtual work δw_{i} in a volume V may, with the above mentioned contributions, be expressed as

$$\delta w_{\mathrm{i}} = \int_V \left[\sigma_{ij}\delta\varepsilon_{ij} + (q_{ij} - s_{ij})\,\delta\varepsilon^{\mathrm{p}}_{ij} + m_{ijk}\delta\varepsilon^{\mathrm{p}}_{ij,k}\right] \mathrm{d}V \tag{1}$$

where σ_{ij} is the Cauchy stress, s_{ij} its deviator and ε_{ij} the total strain. The micro stress q_{ij} and moment stress m_{ijk} are the higher-order work conjugate stresses to the plastic strains $\varepsilon^{\mathrm{p}}_{ij}$ and their gradients $\varepsilon^{\mathrm{p}}_{ij,k}$ respectively. The principle of virtual work reads

$$\int_V \left[\sigma_{ij}\delta\varepsilon_{ij} + (q_{ij} - s_{ij})\,\delta\varepsilon^{\mathrm{p}}_{ij} + m_{ijk}\delta\varepsilon^{\mathrm{p}}_{ij,k}\right] \mathrm{d}V = \int_S \left[T_i\delta u_i + M_{ij}\delta\varepsilon^{\mathrm{p}}_{ij}\right] \mathrm{d}S \tag{2}$$

where δu_i and $\delta\varepsilon^{\mathrm{p}}_{ij}$ vanish on parts of the surface S where u_i and $\varepsilon^{\mathrm{p}}_{ij}$ are prescribed respectively, and where T_i denotes the traction vector and $M_{ij} = m_{ijk}n_k$ the moment traction corresponding to m_{ijk}. An evaluation of the variational principle results in two sets of equilibrium equations

$$\sigma_{ij,j} = 0, \tag{3}$$

$$m_{ijk,k} + s_{ij} - q_{ij} = 0. \tag{4}$$

2.2 *Constitutive equations*

In the most general case one can introduce a free energy per unit volume ψ that depends on both the elastic and plastic strains as well as the plastic strain gradients. The requirement that the dissipation must be non-negative can be expressed using the rate of dissipation which is the difference of the internal work

rate and the rate of change in free energy, hence

$$\int_V \left[\left(\sigma_{ij} - \frac{\partial \psi}{\partial \varepsilon^{\mathrm{e}}_{ij}} \right) \dot{\varepsilon}^{\mathrm{e}}_{ij} + \left(q_{ij} - \frac{\partial \psi}{\partial \varepsilon^{\mathrm{p}}_{ij}} \right) \dot{\varepsilon}^{\mathrm{p}}_{ij} + \left(m_{ijk} - \frac{\partial \psi}{\partial \varepsilon^{\mathrm{p}}_{ij,k}} \right) \dot{\varepsilon}^{\mathrm{p}}_{ij,k} \right] \mathrm{d}V \geq 0. \tag{5}$$

If the Cauchy stress is allowed to depend solely on the elastic strains via the linear elastic stiffness tensor as $\sigma_{ij} = C_{ijkl}\varepsilon^{\mathrm{e}}_{kl}$ then the dissipation condition may be written as

$$\bar{q}_{ij}\dot{\varepsilon}^{\mathrm{p}}_{ij} + \bar{m}_{ijk}\dot{\varepsilon}^{\mathrm{p}}_{ij,k} \geq 0, \tag{6}$$

where

$$\bar{q}_{ij} = q_{ij} - \frac{\partial \psi}{\partial \varepsilon^{\mathrm{p}}_{ij}}, \qquad \bar{m}_{ijk} = m_{ijk} - \frac{\partial \psi}{\partial \varepsilon^{\mathrm{p}}_{ij,k}}. \tag{7}$$

Furthermore, if one assumes that the moment stresses m_{ijk} can be directly determined from the free energy and that the free energy does not explicitly depend on $\varepsilon^{\mathrm{p}}_{ij}$, the dissipation inequality is once again reduced and now takes on a form reminiscent of the standard expression for plastic dissipation except that q_{ij} appears instead of σ_{ij} as

$$q_{ij}\dot{\varepsilon}^{\mathrm{p}}_{ij} \geq 0. \tag{8}$$

It is emphasised that the assumption that the free energy only depends on the gradient of plastic strain is a simplification, and that a more general dependence is discussed by Gudmundson [13]. The flow rule for $\dot{\varepsilon}^{\mathrm{p}}_{ij}$ follows from the standard J_2-theory where the stress deviator is replaced by the microstress q_{ij}. In the special case of a vanishing moment stress m_{ijk}, it is seen from (4) that the microstress q_{ij} is the same as the deviatoric Cauchy stress s_{ij}, and the J_2-formulation is recovered.

Under the assumption that the moment stresses m_{ijk} can be determined directly from a free energy ψ and allowing for an additive decomposition of ψ as,

$$\psi = \psi_{\mathrm{e}}(\varepsilon^{\mathrm{e}}_{ij}) + \psi_{\mathrm{g}}(\varepsilon^{\mathrm{p}}_{ij,k}), \tag{9}$$

the moment stresses will be given as,

$$m_{ijk} = \frac{\partial \psi_{\mathrm{g}}}{\partial \varepsilon^{\mathrm{p}}_{ij,k}}. \tag{10}$$

It is here assumed that the free energy ψ_{g} depend on the plastic strain gradients as

$$\psi_{\mathrm{g}} = \frac{2}{n}\kappa \left(\varepsilon^{\mathrm{p}}_{ij,k}\varepsilon^{\mathrm{p}}_{ij,k} \right)^{\frac{n}{2}}, \tag{11}$$

where $\kappa = G\ell^n$, G is the shear modulus and ℓ is a microstructural length scale. The moment stress then reads,

$$m_{ijk} = 2\kappa \left(\varepsilon^{\mathrm{p}}_{st,q}\varepsilon^{\mathrm{p}}_{st,q} \right)^{\frac{n}{2}-1} \varepsilon^{\mathrm{p}}_{ij,k}. \tag{12}$$

3 Shearing of a laminate

Consider a laminate of two materials, shown schematically in Fig. 1. The plies of material 1 have thickness $2h_1$ and the plies of material 2 have thickness $2h_2$. Each ply has its surface normal parallel to the y-axis.

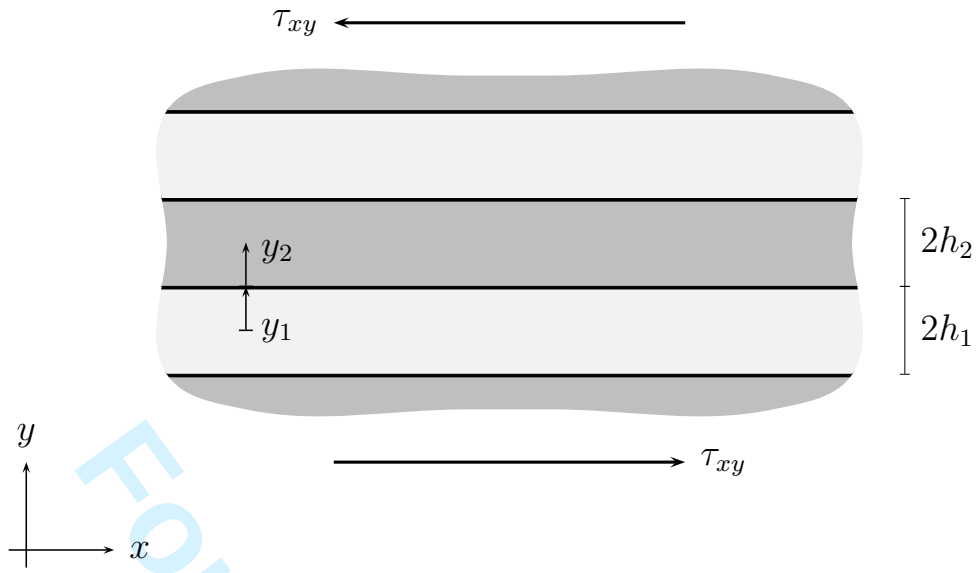

Figure 1. Schematic figure of the laminated structure and loading conditions. (Moment equilibrium is fulfilled, but not shown in figure.)

It will here be assumed that material 1 is softer than material 2 in the sense that it has a lower initial yield stress. Two local coordinates are introduced that are colinear with the global y-axis. In material 1 the coordinate $0 \leq y_1 \leq h_1$ has its origin in the middle of the ply and terminates at the interface, and in material 2 the coordinate $0 \leq y_2 \leq h_2$ varies from the interface to the middle of the ply, hence the two coordinates together describe a repeating element of the laminate such that symmetry can be exploited at the endpoints.

The laminate is assumed to have an infinite extension in the y-direction to avoid edge effects. A pure shear stress $\tau_{xy} = \tau_{yx} = \tau$ is applied to the laminate. Since the two materials are assumed to have different mechanical properties a situation of constrained plastic flow will arise as material 1 starts to yield plastically.

3.1 *Differential equation for plastic shear strains*

The only non vanishing moment stress component is m_{xyy} and it is found from (12) using $2\varepsilon^{\mathrm{p}}_{xy,y} = \gamma'_{\mathrm{p}}$ (where a $(\bullet)'$ denotes differentiation with respect to the spatial coordinate y) as,

$$m_{xyy} = 2^{\left(1-\frac{n}{2}\right)}\kappa\left(\gamma'_{\mathrm{p}}\right)^{n-1}. \tag{13}$$

Combining (4) and (13) yields an expression for the micro stress component

$$q_{xy} = \tau_{xy} + m_{xyy,y} = \tau + 2^{\left(1-\frac{n}{2}\right)}\kappa(n-1)\left(\gamma'_{\mathrm{p}}\right)^{n-2}\gamma''_{\mathrm{p}}. \tag{14}$$

The yield condition is $\Sigma = \sigma_f\left(\varepsilon^{\mathrm{p}}_{\mathrm{e}}\right)$, where Σ denotes the von Mises effective stress measure of q_{ij} and $\varepsilon^{\mathrm{p}}_{\mathrm{e}}$ the effective plastic strain. In this particular case they are

$$\Sigma = \sqrt{3}q_{xy} \tag{15}$$

$$\varepsilon^{\mathrm{p}}_{\mathrm{e}} = \frac{1}{\sqrt{3}}\gamma_{\mathrm{p}}, \tag{16}$$

if a monotonic loading is assumed. The evolution of the flow stress is assumed to be governed by a linear

hardening model,

$$\sigma_f\left(\varepsilon_{\mathrm{e}}^{\mathrm{p}}\right) = \sigma_{\mathrm{s}} + H\varepsilon_{\mathrm{e}}^{\mathrm{p}}, \tag{17}$$

where H is a plastic hardening modulus and σ_{s} is the initial yield stress. The micro stress can also be expressed from (17) as

$$q_{xy} = \tau_{\mathrm{s}} + \frac{H}{3}\gamma_{\mathrm{p}}, \tag{18}$$

where the yield stress in shear is $\tau_{\mathrm{s}} = \sigma_{\mathrm{s}}/\sqrt{3}$. Combining (14) and (18) results in a nonlinear, inhomogeneous second-order differential equation for $\gamma_{\mathrm{p}}(y)$,

$$\gamma_{\mathrm{p}}'' = \frac{2^{\left(\frac{n}{2}-1\right)}}{\kappa(n-1)}\left(\gamma_{\mathrm{p}}'\right)^{2-n}\left(\tau_{\mathrm{s}} - \tau + \frac{H}{3}\gamma_{\mathrm{p}}\right). \tag{19}$$

These equations are found under the assumption of a monotonically increasing load, and if unloading was to be considered then special care would need to be taken, to account for the fact that γ_{p} is a plastic deformation and therefore irreversible in a strict thermodynamical sense.

3.2 *The interface*

Special care is taken to formulate the boundary condition at the interface between two plies. One way to consider different kinds of interface conditions within the frame of strain gradient plasticity is to introduce an interfacial free energy per unit area, Γ, that depends on the plastic strain state at both sides of the interface, cf. Gudmundson [13], Fredriksson and Gudmundson [16].

$$\Gamma = \frac{1}{2m}\left(G_1 L_1\left(\gamma_{\mathrm{p1}}\right)^m + G_2 L_2\left(\gamma_{\mathrm{p2}}\right)^m + \sqrt{G_1 G_2}\, L_3\left(\gamma_{\mathrm{p1}} - \gamma_{\mathrm{p2}}\right)^m\right), \tag{20}$$

where the three L_i are microstructural length scales and m is a constant. The plastic shear strains are evaluated immediately at the interface, but on either side, denoted by the numbers 1 and 2 respectively. The formulation allows for a discontinuity in plastic strains over the interface, and in gradients thereof, but continuity can be restored with an appropriate choice of length scales.

This interface energy formulation is motivated by the fact that at an internal boundary a thin layer of dislocation pileup is usually observed during plastic straining. If the thickness of this zone is much smaller than the material length scale, the energy associated with it can be assumed to hinge only upon the interface itself. This will lead to a contribution to the internal work as

$$\begin{aligned}\delta w_{\mathrm{i}} = {} & \int_V \left[\sigma_{ij}\delta\varepsilon_{ij} + \left(q_{ij} - s_{ij}\right)\delta\varepsilon_{ij}^{\mathrm{p}} + m_{ijk}\delta\varepsilon_{ij,k}^{\mathrm{p}}\right]\mathrm{d}V \\ & + \int_{S_{\mathrm{I}}}\left[M_{ij}^1\delta\varepsilon_{ij}^{\mathrm{p1}} + M_{ij}^2\delta\varepsilon_{ij}^{\mathrm{p2}}\right]\mathrm{d}S_{\mathrm{I}}.\end{aligned} \tag{21}$$

The interfacial moment tractions can then be determined from the interface potential as

$$M_{ij}^I = \frac{\partial\Gamma}{\partial\varepsilon_{ij}^{\mathrm{p}I}} \quad \Rightarrow \quad M_{xy}^I = 2\frac{\partial\Gamma}{\partial\gamma_{\mathrm{p}I}}, \qquad I = 1,2 \tag{22}$$

Using (20), the moment tractions on each side of the interface are

$$\begin{aligned}M_{xy}^1 &= G_1 L_1\left(\gamma_{\mathrm{p1}}\right)^{m-1} + \sqrt{G_1 G_2}\, L_3\left(\gamma_{\mathrm{p1}} - \gamma_{\mathrm{p2}}\right)^{m-1} \\ M_{xy}^2 &= G_2 L_2\left(\gamma_{\mathrm{p2}}\right)^{m-1} - \sqrt{G_1 G_2}\, L_3\left(\gamma_{\mathrm{p1}} - \gamma_{\mathrm{p2}}\right)^{m-1}.\end{aligned} \tag{23}$$

3.3 *Boundary conditions*

Boundary conditions at the interface can be introduced by considering the balance equations at the interface

$$\left.\begin{aligned} m^1_{xyy} + M^1_{xy} &= 0 \\ -m^2_{xyy} + M^2_{xy} &= 0 \end{aligned}\right\} \quad y_1 = h_1; \quad y_2 = 0, \tag{24}$$

which define the state on each side of the interface respectively.

In the stronger material 2 there will be a boundary between the material that is experiencing plastic deformation and the material that is not, this is the elastic-plastic boundary located at $y_2 = y_{\text{ep}}$. This will be true for all monotonically increasing loads up to the point where this boundary has reached $y_2 = h_2$, i.e. the material is experiencing full plastic loading. After full plastic development the plastic strains need to be symmetric with respect to the right boundary. So for increasing loading with $y_{\text{ep}} < h_2$ the boundary conditions will be

$$\gamma_{\text{p2}}(y_{\text{ep}}) = \left.\frac{\mathrm{d}\gamma_{\text{p2}}}{\mathrm{d}y_2}\right|_{y_2=y_{\text{ep}}} = 0, \tag{25}$$

and for a fully developed plastic deformation in material 2 the right boundary condition will be reduced to a simple symmetry condition. The condition of vanishing moment stress at the elastic-plastic boundary results in the condition of vanishing derivative in (25), cf. (22).

3.4 *Analytical solution for quadratic energy*

If the free energy is assumed to depend quadratically on the plastic strain gradients, i.e. $n = 2$ in (11), then the governing differential equation in (19) will be linear and reduces to

$$\gamma''_{\text{p}} = \frac{\tau_{\text{s}} - \tau}{\kappa} + \frac{H}{3\kappa}\gamma_{\text{p}}, \tag{26}$$

which has an analytical solution on the form

$$\gamma_{\text{p}}(y) = A\cosh(\lambda y) + B\sinh(\lambda y) - \frac{R}{\lambda^2}, \tag{27}$$

where $\lambda = \sqrt{\frac{H}{3\kappa}}$, $R = \frac{\tau_{\text{s}}-\tau}{\kappa}$ and A, B should be determined from the boundary conditions. The constant B in the solution for material 1 can be determined directly by considering symmetry as $B_1 = 0$. The other three integration constants can be determined from the interface condition defined in (24) and (25). It is noted that (24) and (25) define four equations for three integration constants. The position of the elastic-plastic boundary y_{ep} will however appear as an additional unknown.

For particular choices of the parameters in the expression for the interface energy (20), the resulting interface conditions will as well be linear and a fully analytical solution can be obtained. In the subsequent calculations it will be assumed that $L_1 = L_2 = 0$ and $L_3 \to \infty$. This corresponds to the following interface conditions:

$$\left.\begin{aligned} \gamma_{\text{p1}} &= \gamma_{\text{p2}} \\ m^1_{xyy} &= m^2_{xyy} \end{aligned}\right\} \quad y_1 = h_1; \quad y_2 = 0. \tag{28}$$

3.5 *Interfacial slip strain*

To account for the change in deformation mechanism, from intragrain dislocation mediated plasticity to intergrain boundary sliding deformation at diminishing length scales, an interface slip displacement is considered. The shear slip distance at the interface is

$$\Delta u = u_2(0) - u_1(h_1). \tag{29}$$

It is here assumed that the relation between slip and shear stress can be expressed as

$$\tau = \tau_{\rm I} + \frac{H_{\rm I}}{\ell_{\rm I}}\Delta u, \tag{30}$$

where $\tau_{\rm I}$ is the interface slip strength, $H_{\rm I}$ an interface hardening modulus and $\ell_{\rm I}$ a characteristic length scale of the interface. The slip will contribute to the total average shear strain by

$$\langle\gamma_{\rm I}\rangle = \frac{2\Delta u}{2h_1 + 2h_2} = \frac{\tau - \tau_{\rm I}}{H_{\rm I}}\frac{\ell_{\rm I}}{h_1 + h_2} \tag{31}$$

at load levels above the interface slip strength, i.e. when $\tau \geq \tau_{\rm I}$. Equation (31) clearly demonstrates that the average plastic shear due to slip increases with decreasing layer thicknesses h_1 and h_2. The contribution to the average plastic shear from strain gradient plasticity shows the opposite behavior, thus a maximum in shear is predicted for increasing layer thicknesses. Hence, it can be expected that a minimum in plastic shear is obtained for some intermediate layer thickness. This corresponds to a maximum in strength for this length scale. Numerical examples will be presented in the next section that demonstrate this effect.

3.6 *The length scales*

There are several different length scales appearing in this paper. There are essentially tree groups of length scales; the bulk material lengths ℓ_1 and ℓ_2, the lengths L_1, L_2 and L_3 related to the interfacial free energy formulation and also the characteristic length scale $\ell_{\rm I}$ of the interface which appears as a consequence of the interface slip formulation. In the current exposition no definite physical meaning has been tied to the length scales and they are so far mainly to be considered as fitting parameters of the theory.

There is however a belief that the length scales can be considered representations of some real and measurable physical quantity of a material. Several lengths appear naturally when considering plasticity on the smaller scales; the length of the Burgers vector, the short and long range interaction distance of dislocations, average obstacle diameter, boundary zone thickness or grain diameter, to name a few possible candidates. It is obvious that more research into this matter is of great importance to the further development of a physically based theory.

The lengths related to the interfacial free energy formulation (20) control the interface behaviour. The interface model can be represented by an mechanical analogy of the interface following Fredriksson and Gudmundson in [16]. This approach clarifies how the three lengths (L_1, L_2, L_3) influence the formulation. In Fig. 2 the mechanical analogy is shown. The higher-order moment stresses and the plastic strains are analogous to tractions and displacements on both sides of the interface, and the lengths L_i are then proportional to the stiffness components k_i.

4 Numerical evaluation

To reduce the number of governing parameters, a dimensionless formulation is considered. This also has the benefit of highlighting the important parameters and recasting them in a more convenient form for the subsequent numerical analysis. The problem is scaled with respect to the properties of the harder material, hence all lengths, moduli, stresses etc. in material 2 are equal to unity. The numerical values used in this

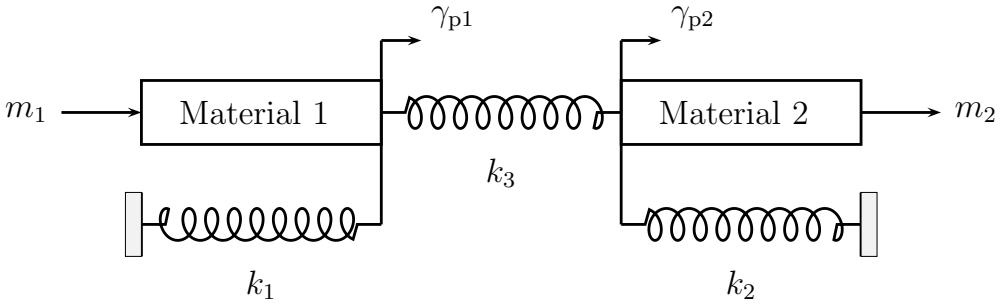

Figure 2. Mechanical analogy of the interface formulation.

Table 1. Length-scale parameters

Parameter[a]	$\bar{\ell}_1$	$\bar{\ell}_I$	$\bar{L}_1$	$\bar{L}_2$	$\bar{L}_3$	h_1/h_2
Numerical value	1	1/10	0	0	∞	1

[a] All lengths are scaled by ℓ_2, except for h_1, for which scaling is shown. Scaling is here indicated by the overscript bar, but will be omitted elsewhere.

Table 2. Moduli and stress parameters

Parameter[b]	$\bar{G}_1$	$\bar{H}_1$	$\bar{H}_2$	$\bar{H}_I$	τ_{1s}/τ_{2s}	τ_I/τ_{2s}
Numerical value	1	1/10	1/10	1/10	1/4	1/3

[b] Shear and hardening moduli scaled by G_2. Indicated here by the overscript bar, but will be omitted elsewhere.

paper are shown in Table 1 and Table 2. Besides these, one more parameter was identified as $\delta = \ell_2/h_2$ which becomes a dimensionless measure of the inverse of the ply thickness.

A monotonically increasing loading in shear is considered and the solution to the governing differential equation can be evaluated numerically to find the plastic strain distribution in the material, see Fig. 3. The elastic strains are calculated by linear elasticity and by applying (31) the average interface slip strains can be found. An averaging procedure is performed for the plastic strains according to

$$\langle \gamma_p \rangle = \frac{1}{h_1 + h_2} \left(\int_0^{h_1} \gamma_{p1} \mathrm{d}y_1 + \int_0^{h_2} \gamma_{p2} \mathrm{d}y_2 \right), \tag{32}$$

and similarly with the elastic strains. The total average strains are then calculated as

$$\langle \gamma_{tot} \rangle = \langle \gamma_e \rangle + \langle \gamma_p \rangle + \langle \gamma_I \rangle. \tag{33}$$

The sum of the average plastic- and interface slip strains are considered to be the total *inelastic* strains. Fig. 4 shows how the inverse of the length scale parameter δ influences the inelastic strains at different shear stresses. It is evident in the figure that there is a distinct minimum in the inelastic strains at some intermediate value of δ. Hence, one can draw the conclusion that this has to correspond roughly to a maximum in yield stress.

An offset yield stress was defined such that the remaining deformation upon unloading would correspond to $0.33\gamma_{s2} = 0.33\tau_{s2}/G_2$. This is quite an arbitrary value, but it is emphasized that it is in the order of, or smaller than, the usual 0.2% offset yield strain commonly used, at least for standard metal alloys. In Fig. 5 the variation of the offset yield strength with the inverse of δ can be seen, and a maximum in offset yield strength is observed.

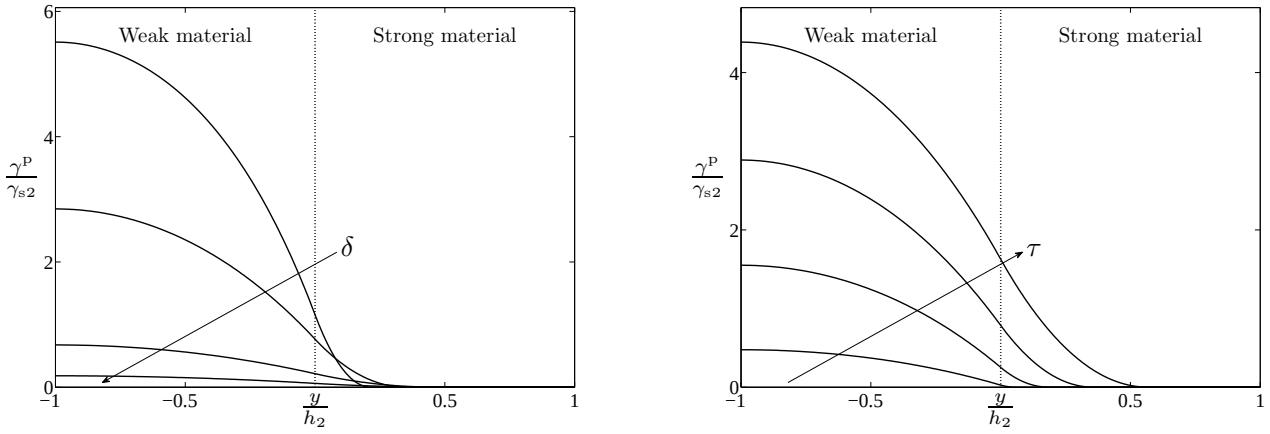

Figure 3. (*Left*) Normalised plastic shear strain distribution evaluated for $\delta = 0.1, 0.2, 0.5, 1$ at a constant load $\tau/\tau_{\mathrm{s}2} = 0.5$. (*Right*) Normalised plastic shear strain distribution evaluated at loads $\tau/\tau_{\mathrm{s}2} = 0.3, 0.4, 0.5, 0.6$ with a constant $\delta = 0.2$. Notice how the plastic shear strains vanishes at the elastic-plastic boundary in the harder material.

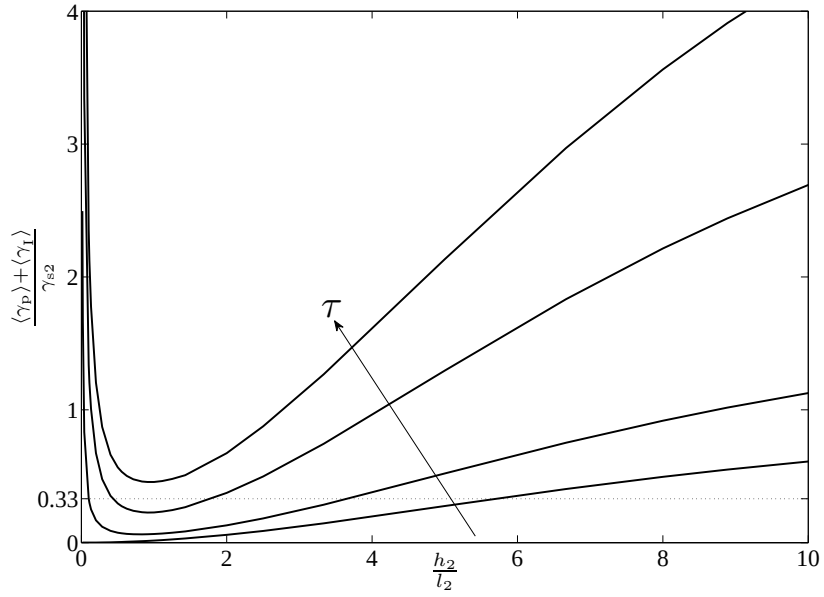

Figure 4. Normalised inelastic strains at loads $\tau/\tau_{\mathrm{s}2} = 0.33, 0.4, 0.6, 0.8$. Notice how the lowest curve corresponds to a load that is less than the interface slip strength, and no slip strain develops.

5 Conclusions

Within a traditional weakest link analysis of the laminate, the yield strength of the weaker material would control how much loading that can be applied before large scale macroscopic yielding would occur. By taking into account the effects of the boundary and the inhomogeneous strain distribution across the plies it has been shown that the ultimate yield strength of the laminate can be increased well beyond this point when the thickness of the plies is decreased relative to some intrinsic material length scale. Adding a interface slip model to the strain gradient theory also revealed that for even smaller thicknesses, relative to the material length scale, the yield strength dropped due to the development of a slip strain at the interface.

The numerical evaluation of the present theory shows a distinct maximum in macroscopic yield strength occurring when competition between the two deformation mechanisms produces a minimum in inelastic

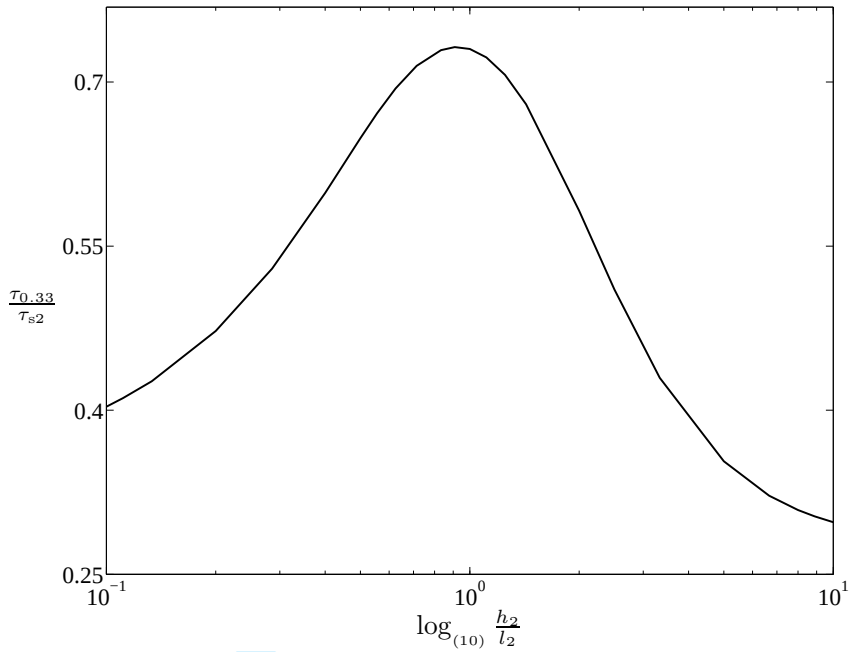

Figure 5. Offset yield strength ($0.33\gamma_{p2}$) for different values on the inverse of δ.

strains. This is in direct analogue with the inverse Hall–Petch effect. There the change from intragrain dislocation mediated plastic deformation is replaced by an intergrain boundary sliding deformation due to a decrease in grain size. It is believed that below a certain grain size the grains can no longer support even a single dislocation loop. It has been shown by molecular dynamics simulations [10] that the majority of deformation activity is expected to occur at the grain boundaries for really small grain diameters, thus strongly indicating a change in deformation mode.

The present theory shows a qualitative representation of both the strain gradient hardening and the inverse Hall-Petch effect. The layer thickness can be thought to be analogous to a grain size. The suggested model for the combination of strain gradient plasticity and grain boundary sliding can be applied to fully three-dimensional formulations of grain structures. The laminate structure was here selected as a simple configuration that still shows the main characteristics of stress–strain behaviour.

Acknowledgment

The authors gratefully acknowledge the Swedish Research Council for financial support under contract 621-2005-5759.

References

[1] N. A. Fleck, G. M. Muller, M.F. Ashby, *et al.*, Acta Metall. Mater. **42** 475 (1994)
[2] J. S. Stölken and A. G. Evans, Acta Mater. **46** 5109 (1998)
[3] H. D. Espinosa, B. C. Prorok and B. Peng, J. Mech. Phys. Solids **52** 667 (2004)
[4] H. Huang and F. Spaepen, Acta Mater. **48** 3261 (2000)
[5] Y. Xiang and J. J. Vlassak, Acta Mater. **54** 5449 (2006)
[6] A. H. Chokshi, A. Rosen, J. Karch, *et al.*, Scripta Metall. **23** 1679 (1989)
[7] H. Conrad and J. Narayan, Acta Mater. **50** 5067 (2002)
[8] M. A. Haque and M. T. Saif, Scripta Mater. **47** 863 (2002)
[9] V. Yamakov, D. Wolf, S. R. Phillpot *et al.*, Nature Materials **3** 43 (2004)
[10] J. Schiøtz and K. W. Jacobsen, Science **301** 1357 (2003)
[11] J. Schiøtz, Scripta Mater. **51** 837 (2004)
[12] G. P. Zheng, Acta Mater. **55** 149 (2007)
[13] P. Gudmundson, J. Mech. Phys. Solids **52** 1379 (2004)

[14] P. Fredriksson and P. Gudmundson, Int. J. Plast. **21** 1834 (2005)
[15] P. Fredriksson and P. Gudmundson, Modelling Simul. Mat. Sci. Eng. **15** 61 (2007)
[16] P. Fredriksson and P. Gudmundson, J. Mech. Phys. Solids **55** 939 (2007)
[17] H. Gao, Y. Huang, W. D. Nix, *et al.*, J. Mech. Phys. Solids **47** 1239 (1999)
[18] Y. Huang, H. Gao, W. D. Nix, *et al.*, J. Mech. Phys. Solids **48** 99 (2000)
[19] N. A. Fleck and J. W. Hutchinson, J. Mech. Phys. Solids **49** 2245 (2001)
[20] M. E. Gurtin, J. Mech. Phys. Solids **50** 5 (2002)
[21] Y. Huang, S. Qu, K. C. Hwang, *et al.*, Int. J. Plast. **20** 753 (2004)

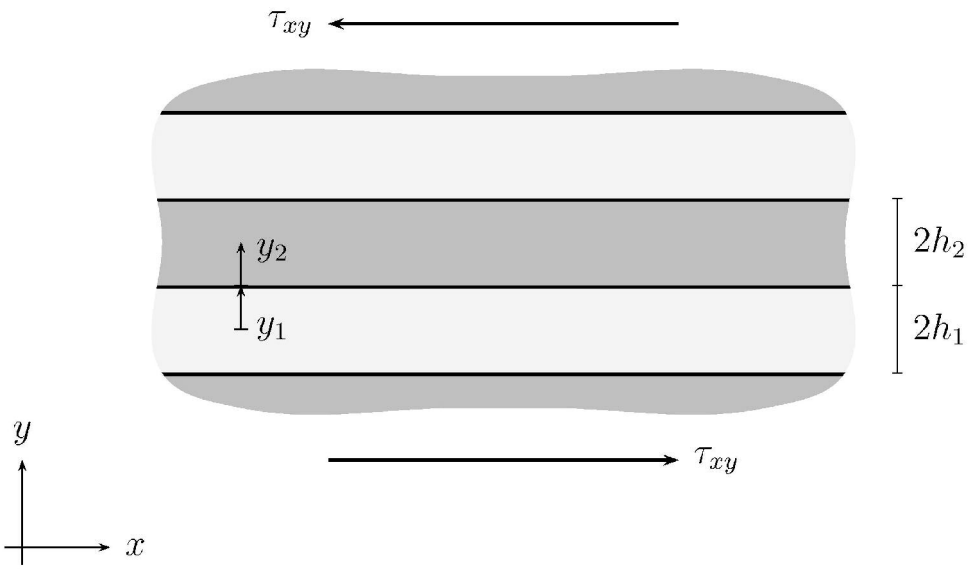

Figure 1
114x68mm (600 x 600 DPI)

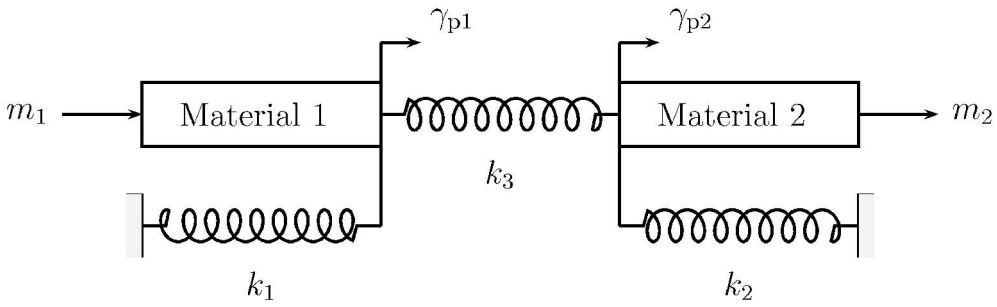

Figure 2
125x38mm (600 x 600 DPI)

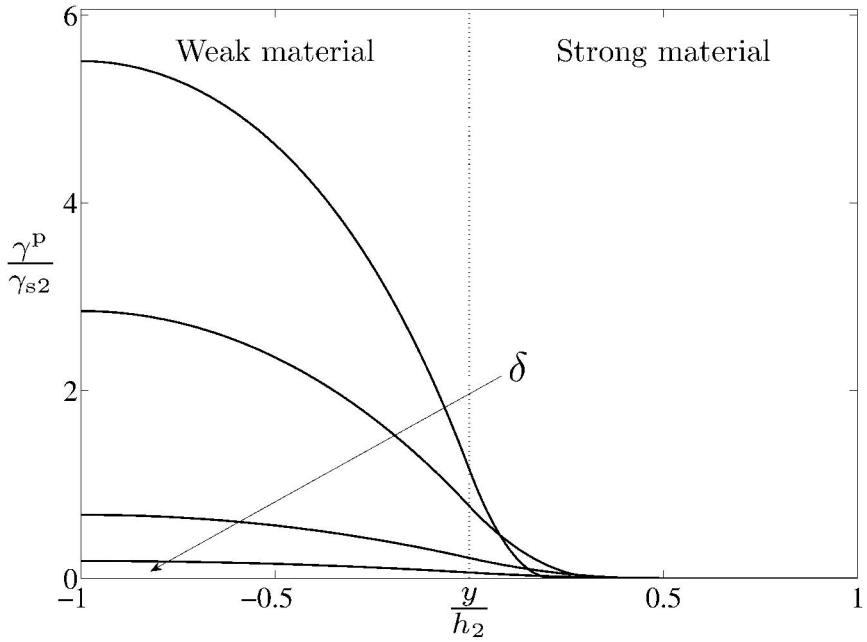

Figure 3a
338x235mm (600 x 600 DPI)

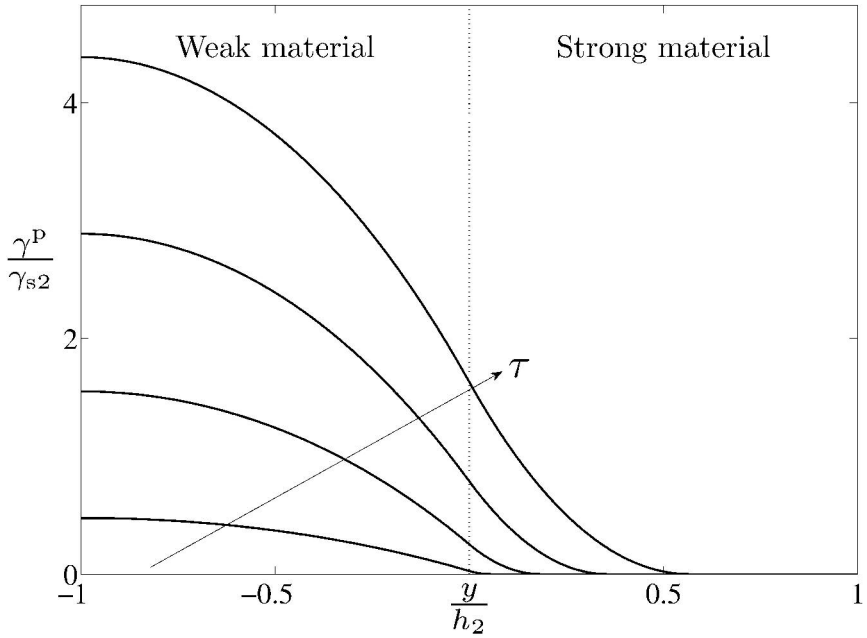

Figure 3b
338x235mm (600 x 600 DPI)

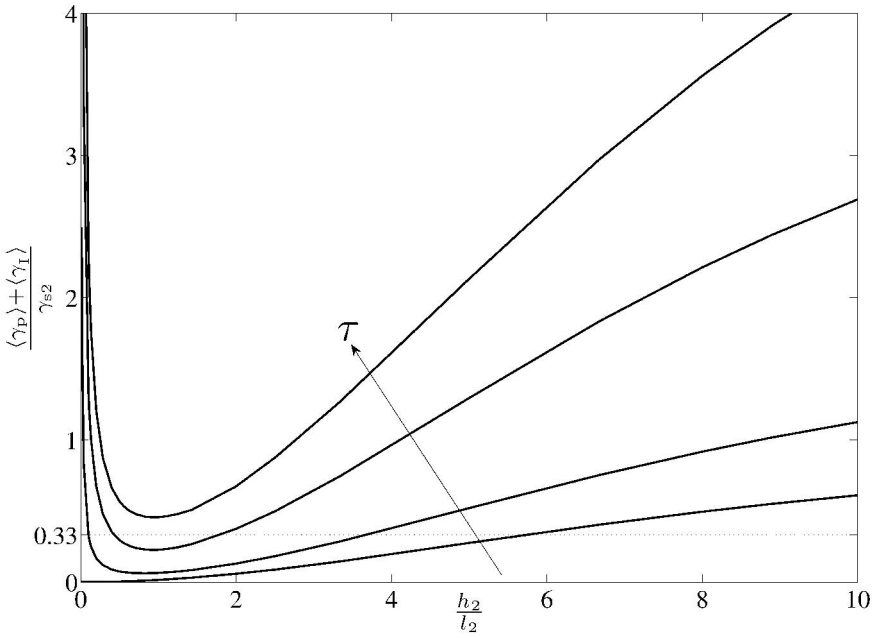

Figure 4
338x235mm (600 x 600 DPI)

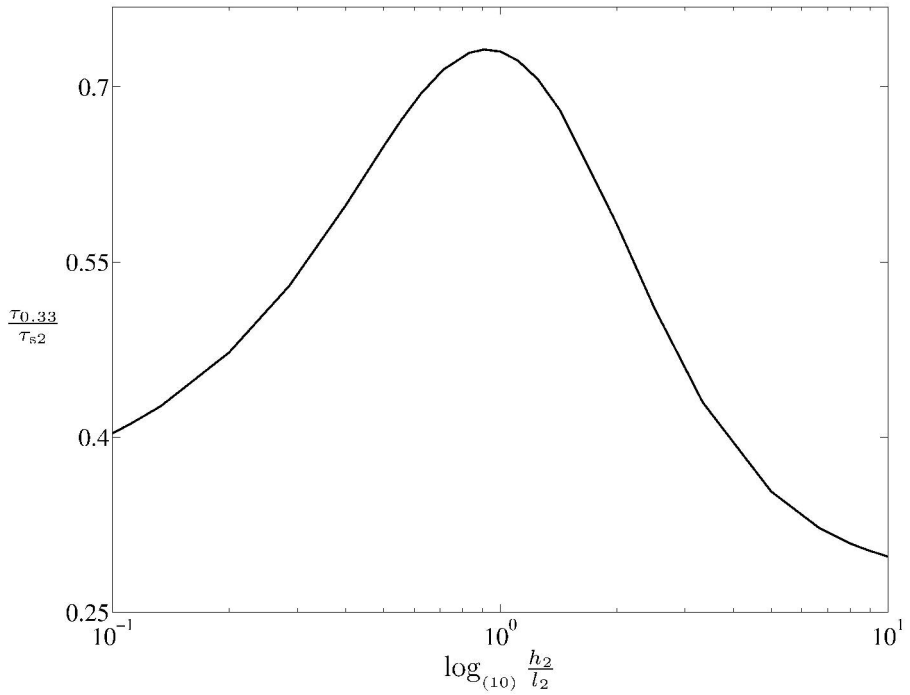

Figure 5
338x251mm (600 x 600 DPI)